View metadata, citation and similar papers at core.ac.uk

brought to you by CORE

provided by Archivio istituzionale della ricerca - Politecnico di Milano

Available online at www.sciencedirect.com

ScienceDirect

Procedia Engineering 167 (2016) 2 – 9

Procedia Engineering

www.elsevier.com/locate/procedia

Comitato Organizzatore del Convegno Internazionale DRaF 2016, c/o Dipartimento di Ing. Chimica, dei Materiali e della Prod.ne Ind.le

Analytical model to describe damage in CFRP specimen when subjected to low velocity impacts

M. Salvetti[a]*, A. Gilioli[a], C. Sbarufatti[a], K. Dragan[b], M. Chalimoniuk[b], A. Manes[a], M. Giglio[a]

[a]*Politecnico di Milano, Department of Mechanical Engineering, Milano, via La Masa 1, 20156, Italy.*
[b]*Air Force Institute of Technology, ul. Ks. Boleslawa 6, 01-494 Warsaw, Poland.*

Abstract

In the light of an increment of the safety of CFRP components subjected to low-velocity impacts, the identification of a damage onset threshold is desired. Hence the suitability of an analytical model for the estimation of the critical load of delamination onset and the resulting delaminated area, as well as for the approximation of the load-displacement curve, has been investigated. The Olsson's analytical model, available in the literature, is considered and applied in this study for the prediction of the mechanical behaviour of composite specimens subject to low-velocity impacts. Comparisons with experimental results have been carried out to demonstrate the accuracy of the presented model. Impact tests were performed in accordance with ASTM D7136 standard and damage was assessed by means of ultrasonic testing and computed tomography.

© 2016 Published by Elsevier Ltd. This is an open access article under the CC BY-NC-ND license (http://creativecommons.org/licenses/by-nc-nd/4.0/).

Peer-review under responsibility of the Organizing Committee of DRaF2016

Keywords: Composite plates; Low-velocity impacts; Delamination; Analitycal model.

1. Introduction

Advanced Composite Materials (ACMs), particularly carbon fiber reinforced plastics (CFRPs), are increasingly replacing conventional aluminum alloys even in primary flight structures as for the Boeing 787 or the more recent

* Corresponding author. Tel.: +39-02-2399-8234.
E-mail address: mauro.salvetti@mail.polimi.it

1877-7058 © 2016 Published by Elsevier Ltd. This is an open access article under the CC BY-NC-ND license (http://creativecommons.org/licenses/by-nc-nd/4.0/).

Peer-review under responsibility of the Organizing Committee of DRaF2016
doi:10.1016/j.proeng.2016.11.662

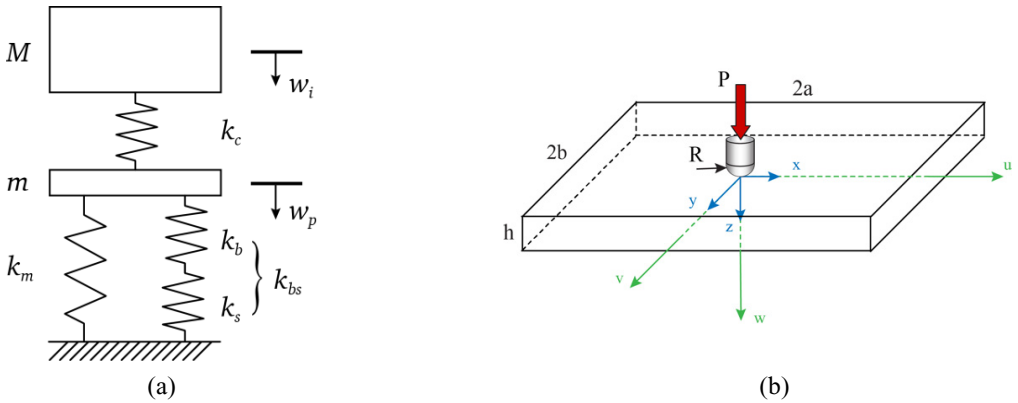

Figure 1: Model for large mass impact (a) and geometry of plate and impactor with nomenclature and reference system (b).

Airbus 350-XWB. This is mainly due to their excellent specific mechanical properties, i.e. higher strength-to-weight and stiffness-to-weight ratios, compared to traditionally used alloys. Moreover, ACMs exhibit improved resistance to corrosion and fire-retardancy, allow considerable flexibility in the design process, thus potentially reducing life cycle costs. However, given the anisotropy and the presence of several possible failure modes, the study of CFRPs result in a not straightforward nor easy task.

A source of major concern, particularly for composite laminates and panels, is their behavior when subjected to loads in the thickness direction, such as impacts. A significant amount of studies has been conducted about the influence of the damage caused by an impact on the residual strength and the fatigue life of the impacted component. More specifically, the damage generated by low-velocity impacts (LVI) is particularly harmful to composite structures as it can significantly degrade their compressive stability and, in general, their structural durability [1], though remaining not easily detectable. The first source for of LVI damage is due to mishandling during manufacturing or maintenance such as, for instance, incidental tool drops. Cyclic loads during flight missions may then contribute to further damage propagation, which may lead to the catastrophic failure of the component. This is one of the reasons why the design approach of primary flight structures, such as fuselage panels and upper wing skins, is usually conservative, thus hampering the weight-saving potential of ACMs. Hence, the development of a reliable analytical model for the prediction of the mechanical behavior of composite structure subject to LVI is of primary importance: indeed, said model could help in reducing time and resources dedicated to experimental testing.

Despite analytical models are often oversimplified, given the high complexities brought by composite materials, some attempts are present in the literature. In particular, major contributions were given by Olsson [2], proposing an analytical model for the prediction of damage initiation and growth regarding large-mass/low-velocity impact. The same author extended the model to small-mass/high-velocity impacts in [3] while a refined closed form approximation for the peak impact load is then used to predict the delamination threshold velocity in [4]. In [5], large-mass impacts on thin ply laminates were investigated: the existing model for quasi-static response is presented and extended to account for damage phenomena observed in thin-ply composites. Huang et Al. [6] established an energy balance for damage development during the impact process with the help of a localized deformation field. Xiao et Al. [7] introduced the initial interlaminar shear strength parameter for the prediction of the interlaminar shear failure due to impact, while the usual simplified energy-balance model and the quasi-static assumption are used to estimate the maximum contact force.

In this study, the capability of the model presented in [2] in predicting a threshold impact load for damage onset and the resulting damage extent, as well as in approximating the load-displacement curve, has been verified and validated experimentally. The analytical model results have been compared with the experimental data, acquired in a similar low velocity impact test configuration as in [2] but employing a different composite material.

2. Experimental Testing

The impact tests [8,9] have been performed by means of a drop test apparatus, which complies with the ASTM D7136 standard. The impactor is instrumented with a Kistler Quartz Force Link Type 9331B (±20kN) so that the impact load history could be recorded. The impact velocity, hence the energy, is acquired by means of a speed trap configuration: two Mikroelektronik M5L/20 lasers are distanced by 41 mm, recording the impactor crossing time. Acquisition is synchronous between all devices with a sampling frequency set to 51.2 kHz. Specimens under consideration comply to the ASTM D7136 standard: 32 unidirectional laminas of Cytec carbon/epoxy system IM7-12k/MTM45-1 were laminated for a total thickness of 4.13mm with a $[(0/45/90/-45)_s]_4$ layup. Laminates were cut out as 150mm long and 100mm wide specimens. Composite material properties are summarized in Table 1 while the experimental program is reported in Table 2.

Table 1: Unidirectional lamina material properties. Courtesy of Cytec Solvay Group.

E_{11} [GPa]	E_{22} [GPa]	G_{12} [GPa]	G_{23} [GPa]	ν_{12}	ν_{23}
157.89	7.65	3.62	3.2	0.361	0.026

Table 2: Experimental program of impact drop-tests.

Impact Energy	4.5 [J]	8.0 [J]	16 [J]	30 [J]
Replicas	2	3	2	2

Non Destructive Testing (NDT) based on ultrasonic (UT) and computed tomography (CT) was necessary for composite damage assessment. In particular, the ultrasonic inspections have been carried out with the automated Boeing (MAUS-V) system. Regarding the computed tomography, specimens have been scanned using the X-ray CT system GE phoenix v|tome|x-m.

3. Analytical modelling of LVI

The proposed model is based on the hypothesis of a long impact duration, thus the plate essentially deforms under static loading (quasi-static hypothesis). As presented in [2], the model is based on the schematic representation in Fig.1a.

The load generated by the contact between the impactor and the plate can be decomposed in three contributions: bending, shear and membrane contribution. For each load component, a corresponding stiffness can be obtained from theoretical formulations referring to a plate with known boundary conditions and defined geometry [2]. Specifically, we can write:

$$P = P_{bs} + P_m \tag{1}$$

where indeed P_{bs} is the sum of the bending and shear load component and P_m is the membrane load component. Defining w_p as the plate transversal displacement under the impactor (Fig.1b), the bending-shear and membrane contributions are

$$P_{bs} = k_{bs} w_p \leq P_{cr} \tag{2}$$

$$P_m = k_m w_p^3 \tag{3}$$

In Eq.(2) the effect of a delamination is modelled by setting a limit on the amount of bending-shear load that the plate can withstand. This threshold critical load depends on the selected number of delaminations n [2] and is defined as

$$P_{cr} = \sqrt{\frac{32\pi^2 D^* G_{IIc}}{n+2}} \tag{4}$$

where D^* is the effective plate stiffness and G_{IIc} is the critical mode II energy release rate. As shown in Fig.2a,

delamination growth is assumed to initiate with a single delamination, $n = 1$, and then increases to a saturation level

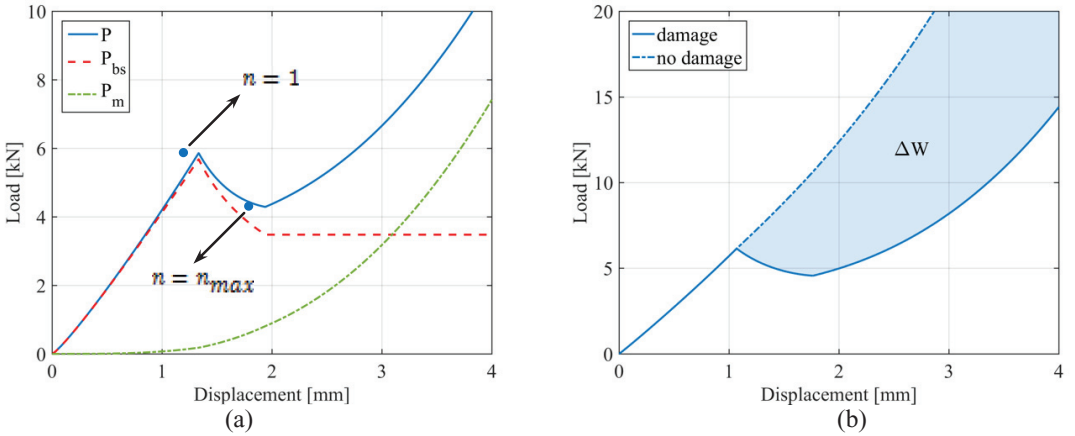

Figure 2: Load-displacement output from the model with impact load decomposed in bending-shear contributions, P_{bs}, and membrane contribution, P_m, (a) and energetic comparison of curves with and without delamination/damage (b).

of delaminations, $n = n_{max}$. Therefore, the critical load of Eq.(4) decreases from an initial level, P_{in}, to a growth level, P_{gr}. Thus, for every j-th transversal displacement level, $w_{p,j}$, we impose that the j-th bending-shear component, $P_{bs,j}$, is equal to

$$P_{bs,j} = \begin{cases} k_{bs,j} w_{p,j} & \text{for } w_{p,j} < w_{in} \\ P_{in}\left(\dfrac{w_{in}}{w_{p,j}}\right) & \text{for } w_{in} \le w_{p,j} < w_{in} \\ P_{gr} & \text{for } w_{p,j} \ge w_{gr} \end{cases} \tag{5}$$

where the initiation and growth levels are

$$P_{in} = P_{cr}(n = 1) \tag{6}$$

$$P_{gr} = P_{cr}(n = n_{max}) \tag{7}$$

and the corresponding displacements are

$$w_{in} = P_{in} / k_{bs,j} \tag{8}$$

$$w_{gr} = P_{gr} / k_{bs,j} \tag{9}$$

The shear stiffness is a nonlinear function of the contact radius r_c, hereafter defined according to Hertzian contact hypothesis. Thus, the indentation α_j has to be calculated iteratively for every j-th level of displacement $w_{p,j}$ since it is function both of the contact radius and the impact load. Starting from a first input value of $0.5h$ for $r_{c,ik}$ and assuming Hertzian contact behavior, α_{ik} is updated at every k-step of the iteration as

$$\alpha_{jk} = \left(\frac{P_{jk}}{k_c}\right)^{2/3} \tag{10}$$

where k_c is the contact stiffness, as formulated in [4], and

$$P_{jk} = P_{bs,jk} + P_{m,jk} \tag{11}$$

$$P_{m,jk} = k_m w_{p,j}^3 \tag{12}$$

with $P_{bs,jk}$ calculated accordingly to Eq.5. The contact radius is updated at every k-step as

$$r_{c,jk} = \sqrt{2R\alpha_{jk}} \tag{13}$$

and the iteration stops when the error, defined as

$$\mathrm{ERR} = |\alpha_{jk} - \alpha_{jk-1}| \tag{14}$$

reaches the imposed threshold of 10^{-6}, empirically selected. Now, since from this model it is possible to estimate a load-displacement curve that considers delamination onset and growth, the work performed by the impactor can also be calculated. Specifically, as presented in [5], the delamination diameter can be obtained considering the load-displacement curves with and without damage as in Fig.2b. With P_0 and P_{dn} the undamaged and damaged plate quasi-static loads, respectively, the energy involved in the damage formation can be expressed as

$$\Delta W = \int_0^{w_{i,max}} (P_0 - P_{dn})\, \mathrm{d}w_i \tag{15}$$

where the displacement of the impactor is $w_i = w_p + \alpha$. Thus the diameter of a circular equivalent damage area, projected in the plane of the laminate, can be calculated as

$$d = 2\sqrt{\frac{\Delta W}{\pi n_{max} G_{IIc}}} \tag{16}$$

4. Results and discussion

The analytical model has been developed in a Matlab framework and it was first verified on the Olsson's data [2]. Then, the same program has been applied to the composite material adopted in the experimental tests [8, 9]. The strain energy release rate G_{IIc} has been assumed equal to $800\ \mathrm{Jm^{-2}}$ which is a reasonable value for a toughened-epoxy matrix as the MTM45-1: for instance, the composite system IM7/8552 exhibits similar values, as reported in [10]. It should be noted that this parameter has a considerable effect not only on the load-threshold for damage onset but also on the estimated delamination diameter. The other parameters influencing the model are the three stiffness parameters k_b, k_s and k_m. These values have been obtained from theoretical formulations derived from the circular plate case and are, in general, approximations. Nonetheless, full clamp boundary condition is considered for the plate and the Hertzian contact hypotheses is valid for little displacements.

4.1. Load-displacement curves

Taking into account these assumptions and looking at Fig.3, the elastic portion of the load-displacement curves is able to reproduce fairly well the experimental results. Specifically, the theoretical load-threshold for damage onset finds correspondence with the drop of the experimental curves, which is typically associated with the first delamination onset [1]. It is however important to remark that such a result is however dependent on the imposed value of G_{IIc}.

After the delamination onset, the experimental curves are compared in Fig.3 with an upper and a lower bound: the upper bound is obtained considering a single delaminated interface, while the lower is established imposing that all the composite layer interfaces with a fiber orientation mismatch withstand de-cohesion during the impact: indeed, delamination occurs between plies of different orientation [1]. For the composite plates considered and, in particular, based on their stacking sequence $[(0/45/90/-45)_s]_4$, a total of 24 interfaces showing an orientation mismatch can be found. Although the upper bound is not exceeded among the different energy levels, the model can no more be considered totally reliable after damage onset. Especially for the higher energy levels, membrane stiffness

degradation might be expected due to significant damage sustained by the plate, as in the form of fiber and matrix failure, while it remains unchanged in the current model. Moreover, for larger displacements, boundary conditions play a significant role in the response, increasing the approximation errors.

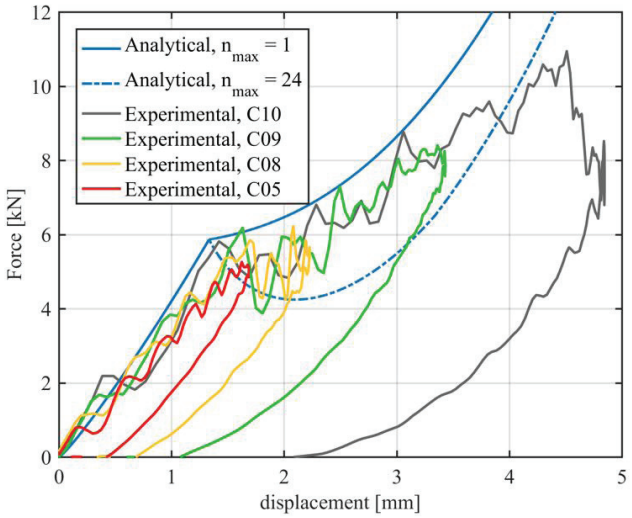

Figure 3: Comparison of analytical and experimental load-displacement (of the impactor) curves for the four tested energy level 4.5J (C05), 8J (C08), 16J (C09) and 30J (C10).

4.2. Diameter of the equivalent circular delamination

Another strong approximation is that the critical load P_{cr} is independent from the shape and the extension of the delamination. The delaminated area is assumed to be circular in [2], thus it is expressed in terms of a diameter. As also shown in Fig.4a based on a computer tomography of a selected impacted specimen, the planar shape of a delamination is far from being circular, though. To overcome this issues, Olsson [2,5] imposed the saturation level of delamination n_{max} equal to the number n^* which represents the amount of equivalent circular delaminations, each with area A_i^*, having the same delamination area A as the total number n of real delaminations (Fig.4b). Thus, for a stack of equally sized delaminations, n/n^* represents the ratio between the actual delamination area and a circular area fully covering the actual delamination. As imposed in [2], supported by fractographic results, Olsson indicated that n^* is 30% of the total interfaces for conventional tape prepreg quasi-isotropic laminates.

For the investigated laminates, this results in a number of equivalent circular delaminations of $n^* \approx 9$. In Fig.5a, the diameter of the delaminated area is show as a function of impact energy for $n^* = 9$ alongside the upper and lower bounds previously defined. The following results can be avowed:

- A threshold impact energy of 3.64J is estimated for delamination damage onset. The identified threshold energy for delamination onset can be considered close to the real experimental behavior as just two very small delaminations have been found in the CT scans of the lower energy test series (4.5J).
- Concerning the top two energy levels (16J and 30J) the analytical model prediction loses validity as, for the equivalent number $n^* = 9$, the actual planar projection of the delaminated area measured by means of UT C-scans is strongly overestimated; if the lower bound (all interfaces delaminated) is considered, although a good match is visible between experimental and analytic results, the model prediction must be interpreted with caution as the delamination work ΔW is calculated from an approximated load-displacement curve. Moreover, all the layout interfaces with orientation mismatch are assumed delaminated and the analytical model approximates all the real delaminations with the same circular area, which is not true as the ultrasonic C-scans testify (Fig.5b). Lastly, as the delamination gets closer to the constrained edges of the plate, boundary condition effects should be also taken into account.

- Regarding the 8J impacts, 21 to 22 delaminated interfaces have been found examining the CT-slices of all three replicas. Thus, considering 40% of the actual number of delaminations, the prediction (for $n^* = 9$) shows good agreement with the experimental results.

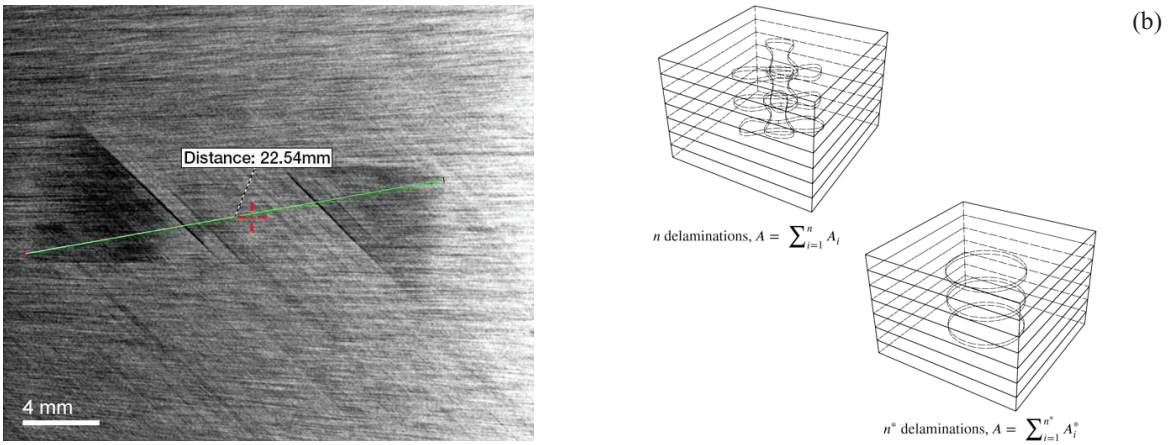

Figure 4: CT slice (a) of specimen C08 (8J impact) of a 90°/-45° interface with visible delamination (darker zones) and matrix cracks (the two darker 45° angled lines). Red crosshair is the impact location. Olsson's approximation (b) of equivalent circular delaminations.

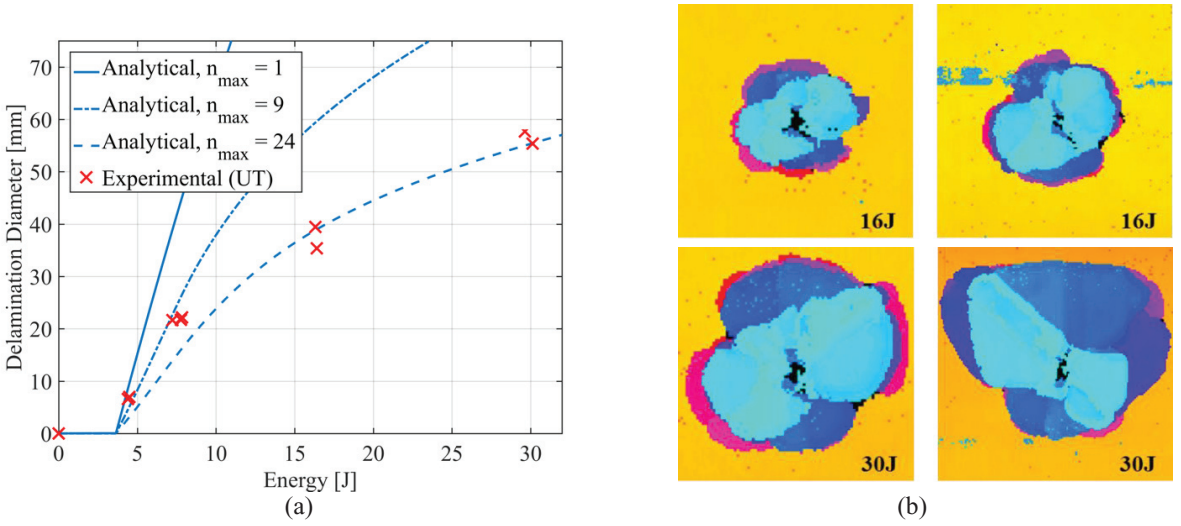

Figure 5: Delamination diameter as a function of impact energy and the number of considered delaminations. Y-axis is equal to the free width of the plate (a). UT C-Scan for 16J and 30J impacts (b).

All these considerations are driven by the chosen strain energy release rate which, as already pointed out, has a substantial influence over the predicted delamination diameter: a decrease of G_{IIc} corresponds to a shift toward left of the curves in Fig.5a and vice versa. However, the main limitation of the model consists in the dependency of the results on the arbitrary number of equivalent circular delaminations: a link with the impact energy is not defined and this undermines the a priori capability of estimating the damage extent without the use of NDT. Thus, applications should be limited only to very low energy levels, for which the curves for different values of n_{max} are closer together, and to threshold-estimation purposes.

Alternatively, the NDT approach can be changed, taking advantage of the 3D damage assessment potentiality of CT: analyzing the 3D reconstructed model, the total delaminated area of the different interfaces can be quantified and not just the planar projection as with UT. Hence, the experimentally estimated area, disregarding its distribution between ply interfaces, can be compared with the predicted one considered as if only a single interface is delaminated, namely for $n^* = 1$.

5. Conclusions

In the present work, an analytical model available in the literature for the prediction of composite material behavior under low velocity impacts has been tailored, verified and validated on a different composite material and various comments on the results have been provided. Olsson's model is proven to be capable of predicting a threshold energy for delamination onset, while it provides less reliable results concerning the damage extent estimation. A threshold energy for damage onset has been obtained for the tested material and it is in good agreement with the experimental evidences.

Future CT scans should verify the prediction, quantifying the delaminated area at different interfaces and not just the planar projection, thus allowing a more precise comparison of the real delaminated area with the analytical estimated value, calculated assuming a single delaminated interface. Additional future work should address the influence of fiber fracture and methods to predict the exact number of delaminations in different layup configurations.

References

[1] S. Abrate, Impact on Composite Structures. Cambridge University Press, 2005.
[2] R. Olsson, “Analytical prediction of large mass impact damage in composite laminates,” *Compos. - Part A Appl. Sci. Manuf.*, vol. 32, no. 9, pp. 1207–1215, 2001.
[3] R. Olsson, “Closed form prediction of peak load and delamination onset under small mass impact,” Compos. Struct., vol. 59, no. 3, pp. 341–349, 2003.
[4] R. Olsson, M. V. Donadon, and B. G. Falzon, “Delamination threshold load for dynamic impact on plates,” Int. J. Solids Struct., vol. 43, no. 10, pp. 3124–3141, 2006.
[5] R. Olsson, “Analytical prediction of damage due to large mass impact on thin ply composites,” Compos. Part A Appl. Sci. Manuf., vol. 72, pp. 184–191, 2015.
[6] K. Y. Huang, a. De Boer, and R. Akkerman, “Analytical Modeling of Impact Resistance and Damage Tolerance of Laminated Composite Plates,” AIAA J., vol. 46, no. 11, pp. 2760–2772, 2008.
[7] S. Xiao, P. Chen, and Q. Ye, “Prediction of damage area in laminated composite plates subjected to low velocity impact,” Compos. Sci. Technol., vol. 98, pp. 51–56, 2014.
[8] A. Gilioli, C. Sbarufatti, M. Dziendzikowski, K. Dragan, A. Manes, M. Giglio, “Impact on CFRP panel with embedded FBG sensors,” ICILSM2016, Turin, Italy, 2016.
[9] C. Sbarufatti, A. Gilioli, M. Dziendzikowski, K. Dragan, A. Manes, M. Frovel, M. Giglio, “Compression after impact (CAI) test on CFRP panels with embedded FBG sensors,” ICILSM2016, Turin, Italy, 2016.
[10] D. D. R. Cartié and P. E. Irving, “Effect of resin and fibre properties on impact and compression after impact performance of CFRP,” *Compos. - Part A Appl. Sci. Manuf.*, vol. 33, no. 4, pp. 483–493, 2002.